Revised MS (JPET/2004/066944)

# A Novel and Potent PARP-1 Inhibitor, 5-chloro-2-[3-(4-phenyl-3, 6-dihydro-1(2H)-pyridinyl)propyl]-4(3H)-quinazolinone (FR247304), Attenuates Neuronal Damage in Vitro and in Vivo Models of Cerebral Ischemia

**Akinori Iwashita[1], Nobuteru Tojo[1], Shigeru Matsuura[1], Syunji Yamazaki[1], Kazunori Kamijo[2], Junya Ishida[3], Hirofumi Yamamoto[3], Kouji Hattori[3], Nobuya Matsuoka[1] and Seitaro Mutoh[1]**

**[1]Medicinal Biology Research Laboratories, [2]Exploratory Research Laboratories, [3]Medicinal Chemistry Research Laboratories, Fujisawa Pharmaceutical Co., Ltd., 2-1-6 Kashima, Yodogawa-ku, Osaka 532-8514, Japan**

JPET Fast Forward. Published on April 9, 2004 as DOI: 10.1124/jpet.104.066944
This article has not been copyedited and formatted. The final version may differ from this version.


**Running title:** Neuroprotection by PARP inhibitor FR247304 on focal ischemia

**Correspondence and proofs should be sent to:**

Name: Akinori Iwashita

Address: Department of Neuroscience, Medicinal Biology Research Laboratories, Fujisawa Pharmaceutical Co., Ltd., 2-1-6 Kashima, Yodogawa-ku, Osaka 532-8514, Japan

Tel: 81-6-6390-1153; Fax: 81-6-6304-5367

E-mail: aki_iwashita@po.fujisawa.co.jp

No. of text pages: 38

No. of tables: 1

No. of figures: 9

No. of references: 40

No. of words in the Abstract: 268

No. of words in the Introduction: 565

No. of words in the Discussion: 1707

**Recommended section:** Neuropharmacology

**Abbreviations:**

PARP-1, poly(ADP-ribose) polymerase-1; FR247304, 5-chloro-2-[3-(4-phenyl-3, 6-dihydro-1(2H)-pyridinyl)propyl]-4(3H)-quinazolinone; 3-AB, 3-aminobenzaminde; PJ34, N-(6-oxo-5,6-dihydro-phenanthridin-2-yl) -N,N-dimethylactamide; DPQ, 3,4-dihydro-5-[4-(1-piperidinyl)butoxy]-1(2H)-isoquinolinone; $H_2O_2$, hydrogen peroxide; MCA, middle cerebral artery; NAD, nicotinamide adenine dinucleotide; NO, nitric oxide; ANOVA, analysis of variance.

JPET Fast Forward. Published on April 9, 2004 as DOI: 10.1124/jpet.104.066944
This article has not been copyedited and formatted. The final version may differ from this version.


**ABSTRACT**

The activation of poly (ADP-ribose) polymerase-1 (PARP-1) after exposure to nitric oxide or oxygen-free radicals can lead to cell injury via severe, irreversible depletion of NAD. Genetic deletion or pharmacological inhibition of PARP-1 attenuates brain injury after focal ischemia and neurotoxicity in several neurodegenerative models in animals. FR247304 (5-chloro-2-[3-(4-phenyl-3, 6-dihydro-1(2H)-pyridinyl) propyl]-4(3H)-quinazolinone) is a novel PARP-1 inhibitor that has recently been identified through structure-based drug design. In an enzyme kinetic analysis, FR247304 exhibits potent and competitive inhibition of PARP-1 activity, with a Ki value of 35nM. Here we show that prevention of PARP activation by FR247304 treatment protects against both ROS-induced PC12 cell injury *in vitro*, and ischemic brain injury *in vivo*. In cell death model, treatment with FR247304 ($10^{-8}$ M to $10^{-5}$ M) significantly reduced NAD depletion by PARP-1 inhibition and attenuated cell death following hydrogen peroxide (100μM) exposure. After 90 min of middle cerebral artery occlusion in rats, poly (ADP-ribosy)lation and NAD depletion were markedly increasd in the cortex and striatum from 1hr after reperfusion. The increased poly (ADP-ribose) immunoreactivity and NAD depletion were attenuated by FR247304 (32 mg/kg, intraperitoneally) treatment, and FR247304 significantly decreased ischemic brain damage measured at 24hr after reperfusion. While other PARP inhibitors such as 3-aminobenzamide and PJ34 showed similar neuroprotective actions, they were less potent *in vitro* assays and less efficacious *in vivo* model compared to FR247304. These results indicate that the novel PARP-1 inhibitor FR247304 exerts its neuroprotective efficacy in vitro and in vivo experimental models of cerebral ischemia via potent PARP-1 inhibition, and also suggests that FR247304 or its derivatives could be attractive therapeutic candidates for stroke and neurodegenerative disease.

JPET Fast Forward. Published on April 9, 2004 as DOI: 10.1124/jpet.104.066944
This article has not been copyedited and formatted. The final version may differ from this version.


Activation of nuclear enzyme poly (ADP-ribose) polymerase **(**PARP) promotes cell death through processes involving energy depletion. Reactive oxygen species (ROS)-mediated damage of DNA can activate PARP (Szabo et al., 1996; Eliasson et al., 1997), and consumes NAD and consequently ATP, culminating in cell dysfunction or necrosis (Ha and Snyder, 1999). In addition, PARP plays a central role in the caspase-independent apoptosis pathway mediated by apoptosis-inducing factor (AIF). Translocation of AIF from the mitochondria to the nucleus is dependent on PARP activation in neurons treated with various DNA-damaging stimuli including hydrogen peroxide (Yu et al., 2002). This cellular suicide mechanism of both necrosis and apoptosis by PARP activation has been implicated in the pathogenesis of ischemic brain injury and neurodegenerative disorders, and PARP inhibitors have been shown to be effective in animal models of stroke, traumatic brain injury and Parkinson's disease (Cosi et al., 1996; Endres et al., 1997; Abdelkarim et al., 2001; LaPlaca et al., 2001; Iwashita et al., 2004).

The brain is particularly susceptible to radical-mediated neuronal damage because of high levels of oxygen consumption, unsaturated fatty acids, and iron stores, combined with low antioxidant resources. Oxidative stress is a critical step in neuronal degeneration, including cerebrovascular injuries like stroke, in neuropathology like Alzheimer's disease, Parkinson's disease and amyotrophic lateral sclerosis (ALS), as well as in a normal aging (Coyle and Puttfarchem, 1993; Facchinetti et al., 1998). For example, ROS formation is increased after permanent and reversible middle cerebral artery occlusion in rats (Nelson et al., 1992; Chan, 1996; Peters et al., 1998). Infarct volume after focal cerebral ischemia is reported to be reduced by overexpressing extracelluar SOD in mice (Sheng et al., 1998) and by the administration of free radical scavengers (Yamamoto et al., 1983; Yang et al.,

JPET Fast Forward. Published on April 9, 2004 as DOI: 10.1124/jpet.104.066944
This article has not been copyedited and formatted. The final version may differ from this version.


2000; Iwashita et al., 2003). Thus, free radicals highly contribute to brain damage, especially following focal cerebral ischemia.

There is a significant increase of extracellular glutamate following stroke that causes neuronal damage through an excitotoxicity process. Increased glutamate in cerebral ischemia activates *N*-methyl-D-aspartate (NMDA) receptors, resulting in increased intracellular calcium concentration and neuronal Nitric Oxide (NO) synthase (nNOS) activation. NO produced by nNOS reacts with superoxide to form the highly toxic peroxynitrite, and both NO and peroxynitrite can cause DNA damage, followed by PARP activation (Zhang et al., 1994). This mechanism of toxicity is supported by the report that PARP activation is markedly diminished in nNOS-deficient mice subjected to middle cerebral artery occlusion-reperfusion (Endres et al., 1998). There are several other sources of ROS such as metabolism of arachidonic acid via the cyclooxygenase and lipoxygenase pathways, oxidation of hypoxanthine and xanthine by xanthine oxidase, and mitochondrial electron transport, which can contribute to the DNA damage and PARP activation (Siesjo et al, 1989).

Direct evidence for the involvement of PARP in the pathogenesis of neuronal damage in stroke models has been reported; ischemic injuries were markedly decreased in PARP (-/-) mice (Eliasson et al., 1997; Endres et al., 1997) and was also attenuated by the treatment of widely-used PARP inhibitor 3-aminobenzamide (3-AB) in wild type mice (Endres et al., 1997). Furthermore, poly (ADP-ribose) formation was detected in both permanent and transient focal ischemia models, and 3-AB, nicotinamide, and a new series of PARP inhibitor such as 3,4-dihydro-5-[4-1(1-piperidynil)buthoxy]-1(2H)-isoquinolinone (DPQ) and PJ34 ameliorated ischemic brain damage as a result of PARP inhibition in the brain (Takahashi et al, 1997; Tokime et al., 1998; Abdelkarim et al., 2001).

JPET Fast Forward. Published on April 9, 2004 as DOI: 10.1124/jpet.104.066944
This article has not been copyedited and formatted. The final version may differ from this version.


We have recently identified FR247304, as a novel potent PARP-1 inhibitor. The purpose of the present study was, first, to evaluate PARP-1 inhibitory activity of FR247304 using enzyme kinetics analysis. The second purpose of the present study was to determine the PARP-1 inhibitory properties and the neuroprotective properties of FR247304 in *in vitro* experimental neuronal cell death models, in which PARP is markedly activated by $H_2O_2$ exposure. Finally, the neuroprotective properties of FR247304 were investigated using transient focal ischemia model in rats. In this model, PARP activation was also assessed by both poly (ADP-ribose) immunohistochemistry and NAD level to clarify the mechanism of the neuroprotective action of this compound. To compare the neuroprotective activity of FR247304 with other known PARP inhibitors, we also evaluated 3-AB and PJ34 in some models as reference.

JPET Fast Forward. Published on April 9, 2004 as DOI: 10.1124/jpet.104.066944
This article has not been copyedited and formatted. The final version may differ from this version.


## Materials and Methods

### Materials

Rat pheochromocytoma PC12 cells were purchased from American Type Culture Collection (Manassas, VA). FR247304 (5-chloro-2-[3-(4-phenyl-3, 6-dihydro-1(2H)-pyridinyl)propyl]-4(3H)-quinazolinone; chemical structure shown in Fig.1) and PJ34 (N-(6-oxo-5,6-dihydro-phenanthridin-2-yl) -N,N-dimethylactamide) were synthesized at Fujisawa Pharmaceutical Co. Ltd. (Osaka, Japan). 3-AB (3-aminobemzamide) was purchased from Sigma-Aldrich (St. Louis, MO). Vitamin E was purchased from Nakarai Tesque (Kyoto, Japan). Hydrogen peroxide (30%), LDH assay kit was from Wako Pure Chemicals (Tokyo, Japan). Tissue culture medium and fetal bovine serum were purchased from Sigma-Aldrich (St. Louis, MO) and tissue culture dishes were from Sumitomo (Osaka, Japan). Recombinant human PARP enzyme was purchased from Trevigen, Inc. (Gaithersburg, MD) and recombinant mouse PARP-2 enzyme was purchased from Alexis Biochemicals (San Diego, CA). Unless otherwise stated, all other materials were purchased from Sigma-Aldrich (St. Louis, MO).

### Measurement of PARP inhibitory activity and specificity of FR247304

***PARP inhibitory activity in vitro:*** To assess the PARP-1 or PARP-2 inhibitory activity of FR247304, 3-AB and PJ34, PARP activity was evaluated as previously described (Banasik et al., 1992) with minor modifications. PARP enzyme assay was carried out in a final volume of 100µl consisting of 50mM Tris-HCl (pH8.0), 25mM $MgCl_2$, 1mM dithiothreitol, 10µg activated salmon sperm DNA, 0.1µCi of [adenylate-$^{32}$P]-NAD, 0.2 units of recombinant human PARP for PARP-1 assay or 0.1

JPET Fast Forward. Published on April 9, 2004 as DOI: 10.1124/jpet.104.066944
This article has not been copyedited and formatted. The final version may differ from this version.


units of recombinant mouse PARP-2 for PARP-2 assay and various concentrations of FR261529 or 3-AB. The reaction mixture was incubated at room temperature (23°C) for 15min, and the reaction was terminated by adding 200μl of ice cold 20% trichloroacetic acid (TCA) and incubated at 4°C for 10min. The precipitate was transferred onto GF/B filter (Packard Unifilter-GF/B) and washed three times with 10% TCA solution and 70% ethanol. After the filter was dried, the radioactivity was determined by liquid scintillation counting.

***Determination of radical scavenging activity:*** For measurement of lipid peroxidation, thiobarbituric acid reactive substances (TBARS) were estimated using the modified method of Buege and Aust (1978) and Callaway et al. (1998). Briefly, brain synaptosomes were prepared from Wistar rats (from Charles River, Hino, Japan). To evaluate the inhibitory activity of FR247304, different concentrations of the compounds was dissolved 50% dimethyl sulfoxide (DMSO), and then 5μl of diluted solution (the final is 1% DMSO) were added to each rat brain synaptosome and incubated with ammonium ferric sulfate (100 μM) at 37°C for 30min. The reaction was stopped with addition of 20% TCA, and the precipitated proteins were removed by centrifugation at 10,000g for 15min. The aliquots of supernatant were then added to an equal volume of thiobarbituric acid. The samples were heated at 95°C for 30 min, and then cooled on ice before reading absorbance at 532 nm. Concentrations of TBARS were calculated using standard curve obtained with malondialdehyde (MDA). Percent inhibition of TBARS production was calculated as follows: % inhibition =[(Max - Drug)/(Max - Base)] x 100, where Max is the values in the presence of ammonium ferric sulfate, Base is the values in the absence of ammonium ferric sulfate and Drug is the values of test compounds.

***Determination of NOS inhibitory activity:*** NOS catalytic activity was

JPET Fast Forward. Published on April 9, 2004 as DOI: 10.1124/jpet.104.066944
This article has not been copyedited and formatted. The final version may differ from this version.


assayed by measuring the $Ca^{2+}$-dependent conversion of [$^3$H]-arginine to [$^3$H]-citrulline as described by Huang et al. (1993). For this assay, dissected rats brain was homogenized in 20 vol (wt/ vol) of 25mM Tris buffer (pH7.4) containing 1mM EDTA and 1mM EGTA. After centrifugation (20,000 x g for 15 min at 4°C), 25 µl of supernatant was added to 75 µl of 50mM Tris buffer (pH 7.4) containing 1mM NADPH, 1mM EDTA, 3mM $CaCl_2$, and 0.1µCi of [$^3$H] arginine (specific activity 64Ci/mmol; NEN) in the absence or presence of FR247304 solution and incubated for 15 min at 37°C. The reaction was terminated by the addition of 250µl Dowex AG50WX-8 (Pharmacia) and cooled on ice. After centrifugation, [$^3$H]citrulline was quantified by liquid scintillation counting of 100 µl supernatant. No significant [$^3$H]citrulline production occurred in the absence of calcium.

**Preparation of nuclear extracts from PC12 cells and the rat/mouse brain**

For preparation of nuclear extracts, the published methods were used for preparation of nuclear extracts, with minor modifications (Lahiri and Ge, 2000). To prepare the nuclear extracts from PC12 cells, 2 x $10^6$ cells cultured in F25 flask were washed with 10mL of PBS (phosphate buffered saline) and cells were re-suspended in 500µL of cold buffer A (10mM HEPES pH7.6, 15mM KCl, 2mM $MgCl_2$, 0.1mM EDTA, 0.1%NP40) and homogenized gently. The homogenate was centrifuged at 5000g for 30 seconds and the supernatant containing cytoplasm and RNA was removed. The nuclear pellet was re-suspended in 50µL of ice-cold buffer B (50mM HEPES pH7.9, 400mM KCl, 0.1mM EDTA, 10% Glycerol). The tube was mixed thoroughly and placed on a micro tube mixer for 15 min at 4°C. The nuclear extract was centrifuged at 11000g for 10 min. The supernatant containing the proteins from the nuclear extract was removed carefully to a fresh tube. The protein was measured

JPET Fast Forward. Published on April 9, 2004 as DOI: 10.1124/jpet.104.066944
This article has not been copyedited and formatted. The final version may differ from this version.


in the nuclear extract and then used for the PARP-1 assay immediately.

For preparation of nuclear extracts from rat and mouse brain, normal whole brains were dissected and transferred to Teflon homogenizer. The buffer A was added at 300 mg brain tissue per 1mL and ten strokes of homogenization were performed. The whole suspension was transferred equally to the Eppendorf tubes followed by centrifugation in a microcentrifuge (1600g) in a microcentrifuge at 4°C for 1 min. The supernatant contains mostly cytoplasmic constituents were removed, and 300μL of buffer B was added to the nuclear pellet in each of the Eppendorf tubes. The tubes were mixed thoroughly and placed on a micro tube mixer for 15 min. The supernatant containing the proteins from the nuclear extract was removed carefully to a fresh tube. The protein was measured in the nuclear extract and then the crude-solution containing PARP enzyme and DNA was used for the PARP-1 assay immediately.

**Neuroprotective efficacy in PC12 cells**

***Cells and hydrogen peroxide treatment:*** PC12 cell cultured were grown in Dulbecco's modified Eagle's medium supplemented with 5% (v/v) fetal calf serum, 5% (v/v) horse serum, and a 1% (v/v) penicillin-streptomycin antibiotics mixture. Cells were grown in an atmosphere of 95% air and 5% $CO_2$ at 37°C. For all experiment, cells were seeded at a density of $4x10^4$cells/well in 96 well culture plates and allowed to attach overnight.

***Drug treatment:*** FR247304 or PJ34 was dissolved in 100% DMSO at $10^{-2}$ M and then diluted in DMEM without serum. 3-AB was dissolved in 10% DMSO at 1M and then diluted in DMEM without serum. Each solution was added to culture plate 0.5h before $H_2O_2$ exposure.

JPET Fast Forward. Published on April 9, 2004 as DOI: 10.1124/jpet.104.066944
This article has not been copyedited and formatted. The final version may differ from this version.


***Determination of cellular NAD level:*** To determine NAD level in cultured cells, PC12 cells were seeded at $2x10^5$ cell / well in 24 well plates and cultured for 24hrs. FR247304 was added to cell media at several concentrations. Thirty min later, cells were exposed 100μM $H_2O_2$ for 30min and cells were detached using by cell scraper and then collected in microcentrifuge tube by centrifugation for 5 min x 100 g at 4°C. To quantify the NAD level in rat brain, brain homogenate (10 mg tissue/ 150μl in PBS) dissected from the cerebral cortex and the striatum were prepared, respectively. Cells or brain homogenate were extracted with 200μL of 0.5M $HClO_4$ for 15 min, and then 60μL of 2M KOH/0.2M $K_2HPO_4$-$KH_2PO_4$ pH7.5 was added to the acidic supernatant obtained by centrifugation. NAD level in the supernatant was measured using enzymatic conversion to NADH by alcohol dehydrogenase.

***Determination of Cell viability:*** For assessment of cell viability, hydrogen peroxide-induced cytotoxity was quantified by a standard measurement of lactate dehydrogenase (LDH) release with the use of the LDH assay kit (Wako, Japan). Briefly, 6hr after hydrogen peroxide exposure, 20μl medium of each well was collected and the solution prepared from LDH assay kit was added. After incubation at room temperature for 30 min, the reaction was stopped by addition of 1N HCl and absorbance was measured at 450 nm using a microplate reader (Molecular Devices, Sunnyvale, CA).

**Pharmacokinetic study in rats**

Measurement of the concentration of FR247304 in plasma and brain were performed in rats following intraperitoneal administration at 32mg/kg. FR247304 was suspended in 0.5% methylcellulose because it was not soluble in saline, and administered i.p. in a volume of 2mL/kg. The plasma and brain was collected at 0.5, 1,

JPET Fast Forward. Published on April 9, 2004 as DOI: 10.1124/jpet.104.066944
This article has not been copyedited and formatted. The final version may differ from this version.


2, 4, 6hr after dosing, and the plasma and brain level of FR247304 were measured using high-performance liquid chromatography.

**Focal Cerebral Ischemia Models in Rats**

***Animals:*** For transient focal ischemia, 9-10-week-old male Wistar rats weighting 274-380 g from Charles River (Hino, Japan) were used. All animals were housed in a room maintained at 23 ± 2°C with 55 ± 5% humidity, and with a 12-hour light/dark cycle (light on at 07:00). The minimum quarantine period was at least 1 week before the experiment. Animals were housed five per cage and allowed free access to food and water. All experiments in the present study were performed under the guidelines of the Experimental Laboratory Animal Committee of Fujisawa Pharmaceutical Co., Ltd. and were in strict accordance with the principles and guidelines of the National Institutes of Health Guide for the Care and Use of Laboratory Animals. All efforts were made to minimize both the number of animals used and stress to the animals during experimental procedures.

***Laser Doppler flowmetry:*** Changes of regional cerebral blood flow (rCBF) were recorded at the surface of the right parietal cortex using a laser-Doppler flowmetry (Omegaflow, FLO-N1, Neuroscience, Osaka, Japan) before, during and after MCA occlusion. After rats were placed in a stereotaxic frame, craniectomy (2-mm in diameter, 4-6 mm lateral and 1-2 mm caudal to the bregma) was performed with extreme care over the MCA territory. The dura was left intact. The probe of the laser-Doppler flowmeter was lowered to the bottom of the cranial burr hole using a micromanipulator. The probe was held stationary by a probe holder secured to the skull with dental cement. Changes in rCBF were expressed as a percentage of the baseline value.

JPET Fast Forward. Published on April 9, 2004 as DOI: 10.1124/jpet.104.066944
This article has not been copyedited and formatted. The final version may differ from this version.


***Transient Focal Ischemia in Rats:*** Transient occlusion of the right MCA was induced by insertion of a nylon suture through the right internal carotid artery to the origin of the MCA as previously described (Furuichi et al., 2003). Rats were anesthetized with a mixture of 4.0% halothane and oxygen-nitrogen (30% oxygen and 70% nitrogen), and maintained with a mixture of 1.5% halothane and oxygen-nitrogen during the procedure. Each animal was placed in the supine position, and a midline incision was made to the skin of the neck. The right common carotid artery (CAA) was exposed with careful protection of the vagus nerve. The external carotid artery (ECA), internal carotid artery (ICA), and CCA were carefully isolated and maintained in a 'Y' shape by use of silk suture. After ligation of the ECA and CCA, an incision to insert a monofilament was made at the bifurcation. The monofilament was a 19-mm-long, 4-0nylon surgical suture (Nicchou, Tokyo, Japan) coated with silicone (Xantopren L, Heraeus Kulzer, Dormagen, Germany) to thicken the distal 5 mm to about 0.4 mm in diameter. The proximal tip of the monofilament was heated to create a globular stopper for easy removal. The monofilament was introduced into the lumen of the ICA. In this way, the monofilament passed through the origin of the MCA and thereby occluded it. A silk suture was toed around the ICA to immobilize the monofilament. The neck wound was closed and each animal was allowed to recover from anesthesia. Ninety minutes after MCA occlusion, each animal was re-anesthetized, and the neck wound was re-opened to remove the monofilament and to resume blood flow to the MCA. The neck wound was closed again.

***Drug administration:*** FR247304, PJ34 or 3-AB, which was suspended with 0.5% methylcellulose, was administered at doses of 10 and 32 mg/kg for FR247304, 3.2 and 10mg/kg for PJ34 or 32 and 100mg/kg for 3-AB intraperitonially twice at 10min prior to MCA occlusion and 10min prior to recirculation. The administration

JPET Fast Forward. Published on April 9, 2004 as DOI: 10.1124/jpet.104.066944
This article has not been copyedited and formatted. The final version may differ from this version.


volume was adjusted to 2ml/kg.

***Measurement of Brain damage:*** Twenty four hrs after the reperfusion, each rat was anesthetized with intraperitoneal administration of sodium pentobarbital (50mg/kg) and the brain was fixed by transcardial perfusion with heparinized saline and then with 10% neutral formalin solution. The brain was cut into 2-mm coronal slices using a brain microslicer at +4, +2, 0, -2, -4 and -6mm from the bregma. Each coronal slice was embedded in paraffin and 3 to 4 μm sections were prepared from each slice with a microtome. These sections were stained with hematoxylin and eosin. To correct swelling due to brain edema or atrophy caused by tissue damage, the damaged area was compensated by the ratio of the whole area of the left cerebral hemisphere to that of the right cerebral hemisphere. The area with ischemia brain damage was delineated under light microscopy and quantified using an image analyzer system. The total damaged area was determined by summing up the damaged area from the six sections and presented as percentage of the damaged area compared to the whole coronal area.

***Determination of NAD content in rat brain:*** The NAD level in the cortex and striatum after ischemia-reperfusion in rats were quantified as described above. For time course study, the brain was removed at 0, 1, 3 and 24hr after reperfusion and cut into 2-mm coronal slice using a brain microslicer at 0 mm from the bregma. The cerebral cortex and striatum of damaged hemisphere were carefully dissected and the NAD level was quantified as described above. To evaluate the effect of FR247304, the cerebral cortex and striatum of damaged hemisphere were dissected at 3hr after reperfusion.

***Poly (ADP-ribose) immunohistochemistry:*** To detect the distribution of poly (ADP-ribosyl)ation after focal brain ischemia, rats were anesthetized with sodium

JPET Fast Forward. Published on April 9, 2004 as DOI: 10.1124/jpet.104.066944
This article has not been copyedited and formatted. The final version may differ from this version.


pentobarbital (50mg/kg) and transcardially perfused with 4% paraformaldehyde at 1 and 6hr after induction of ischemia. After immediate removal, brains were stored in the buffer containing 20% sucrose overnight at 4°C. Frozen coronal sections (40μm) were prepared on a freezing microtome and then endogenous peroxidase was quenched in 0.3% $H_2O_2$ in methanol. After blocking with 10% donkey serum, sections were incubated with rabbit anti-poly (ADP-ribose) polyclonal antibody (BIOMOL) at 4°C overnight. This antibody was used at a concentration of 1:100. The sections were washed with 0.05% Triton-X in phosphate-buffered saline, and then incubated with biotinylated goat anti-rabbit IgG antibody at 1:150 dilutions for 30min and with a peroxidase-streptavidin for 30min. Peroxidase was developed with AEC (Santa Cruze Biotechnology, Inc.) for 30min and colored red. Finally, to enhance nuclear staining, the sections were counterstained with hematoxylin (blue color).

**Statistical analysis**

The $IC_{50}$ values obtained from studies in vitro were calculated using GraphPad Prism 3.3 software (GraphPad Software, Inc., San Diego, CA). All values are expressed as mean ± S.E.M. Statistical analysis was carried out using Student's t-test comparing the drug-treated group with control group and by using one-way analysis of variance (ANOVA) followed by Dunnett's multiple comparison test for the drug-treated groups versus the control group. P-value less than 0.05 was considered to be significant.

JPET Fast Forward. Published on April 9, 2004 as DOI: 10.1124/jpet.104.066944
This article has not been copyedited and formatted. The final version may differ from this version.


## Results

### Enzyme kinetics study and PARP-1/ PARP-2 inhibitory activity of FR247304

FR247304 exhibited typical competitive inhibition of enzyme kinetics (Fig.2A) with a Ki value of 35nM (Fig. 2B). To compare the species differences of PARP inhibitory activity of FR247304, human recombinant PARP and nuclear extract from rat and mouse brain were used as rat PARP and mouse PARP-1. FR247304 potently inhibited the enzyme activity with an $IC_{50}$ of 65 ± 0.9 nM, 68 ± 2.1 nM and 63 ± 1.8 nM in human, rat and mouse PARP, respectively (Fig. 3A). To compare PARP inhibitory activity with other well-known PARP inhibitors, 3-AB and PJ34 were also evaluated. They inhibited the PARP enzyme activity with an $IC_{50}$ of 11200 ± 810 nM and 110 ± 1.9 nM, respectively (Table 1). Furthermore, to confirm the selectivity of FR247304, PARP-2 enzyme assay was also conducted. In our assay system, FR247304 was shown to be about 10-fold selective to PARP-1 ($IC_{50}$ value was 68 nM) than PARP-2 ($IC_{50}$ value was 620 nM).

### Specificity of FR247304

To determine whether FR247304 has properties to reduce the ROS-induced cytotoxicity directly, radical scavenging activity and NOS inhibitory activity were evaluated using TBARS assay and NOS catalytic activity assay. FR247304 did not inhibit TBARS production even at a concentration of $10^{-5}$M, although vitamin E showed radical scavenging activity from $10^{-6}$M (Fig. 3B). In the NOS assay, 7-nitroindazole, a selective nNOS inhibitor, prevented NOS catalytic activity assessed by [$^3$H]-citrulline production at the concentrations ranging from $10^{-7}$ M to $10^{-5}$ M although FR247304 had no inhibitory activity up to $10^{-5}$M (Fig. 3C). Thus, these

JPET Fast Forward. Published on April 9, 2004 as DOI: 10.1124/jpet.104.066944
This article has not been copyedited and formatted. The final version may differ from this version.


results suggest that FR247304 can potently and competitively inhibit PARP enzyme and has no properties to scavenge the free-radicals and to inhibit the NOS activity.

**Neuroprotective action in PC12 cells**

In this *in vitro* study, we confirmed whether $H_2O_2$ treatment induced PARP activation, as well as concomitant NAD depletion and cell death in rat pheochromocytoma PC12 cells. PARP activation by $H_2O_2$ exposure was evaluated by NAD assay. Excessive PARP activation by $H_2O_2$ (100 μM) exposure for 30min resulted in massive NAD depletion (Fig.4A), and this NAD depletion was concentration-dependently inhibited by FR247304 treatment ($10^{-8}$M to $10^{-5}$M). Furthermore, exposure of $H_2O_2$ for 6hr induced severe cell damage, although FR247304 treatment at a concentration ranging from $10^{-8}$M to $10^{-5}$M significantly and concentration-dependently attenuated cell death assessed by LDH release assay (Fig.4B). To compare the neuroprotective properties of other PARP inhibitors in PC12 cells, 3-AB and PJ34 were evaluated using by LDH assay. 3-AB and PJ34 treatment also significantly and concentration-dependently attenuated cell death at a concentration ranging from $10^{-4}$M to $10^{-2}$M and $10^{-7}$M to $10^{-5}$M, respectively (Table 1).

**Pharmacokinetic study**

The plasma and brain concentrations of FR247304 in rats were determined at 0.5, 1, 2, 4 and 6hr following intraperitoneal administration at 32 mg/kg. Mean plasma and brain concentrations of Cmax were 0.15μg/ml and 0.74μg/g tissue, respectively, and even at 6hr after dosing, the plasma and brain concentration were relatively highly sustained (0.10 μg/mL in the plasma and 0.36μg/g tissue in the brain) as shown in Fig. 5. Thus, the concentration of FR247304 in the brain was significantly higher

JPET Fast Forward. Published on April 9, 2004 as DOI: 10.1124/jpet.104.066944
This article has not been copyedited and formatted. The final version may differ from this version.


than that in the blood and the brain/plasma concentration ratio was 4.35 at the Cmax time point (1h after dosing).

**Neuroprotective action of FR247304 in rat focal cerebral ischemia**

***Effect of FR247304 on ischemic damage after transient focal cerebral ischemia:*** Regional cerebral blood flow (rCBF) decreased to 21.3 ± 3.7 % (n=9) of the baseline level immediately after MCA occlusion and sustained during 90min of ischemia in the control group. After reperfusion, rCBF increased to 95% to 100% of baseline within 5 minutes. FR247304 (10 and 32 mg/kg, i.p.) did not alter rCBF; rCBF was 21.9 ± 4.6 % (n=9) of the baseline level immediately after the MCA occlusion and was 95% to 100% of baseline after reperfusion. In the control group, the dorsolatelal cortex and basal ganglia showed extensive damage that could be clearly differentiated from normally perfused area (Representative pictures were shown in Fig. 6A). The volume of ischemic brain infarction in the cerebral cortex and striatum in the control group was 126.85 ± 15.58 and 52.64 ± 1.98 $mm^2$, respectively. FR247304 dose-dependently reduced the size of infarcted cortical area when administered 10min prior to MCA occlusion and 10min prior to reperfusion (Fig. 6 B&C). Cortical damage was reduced by 27% and 47% at the doses of 10 and 32 mg/kg, respectively, and the protection at the dose of 32 mg/kg was statistically significant both in total cortical infarct size and in the area at serial coronal sections (2-mm sections 2 to 4) compared to control group ($P<0.05$ by one-way ANOVA followed by Dunnett's multiple comparison test). In the striatum, FR247304 slightly but significantly reduced striatal infarct size by 14% compared with control group. As shown in Fig. 7, MCA occlusion resulted in an increase of body temperature. However, FR247304 treatment had no influence on body temperature both at 1.5hr after occlusion and at 24hr after

JPET Fast Forward. Published on April 9, 2004 as DOI: 10.1124/jpet.104.066944
This article has not been copyedited and formatted. The final version may differ from this version.


reperfusion. To compare the potency and efficacy with other PARP inhibitors, 3-AB and PJ34 were evaluated at a dose of 100mg/kg or at the doses of 3.2 and 10mg/kg, respectively. Cortical damage was slightly reduced by 11% with 3-AB treatment. PJ34 at the dose of 3.2mg/kg significantly reduced cortical damage by 33%, however, 10mg/kg dosing showed reversed effect (17% reduction) (Table 1).

***Poly (ADP-ribose) polymer formation and effect of FR247304:*** Increased immunoreactivity for poly (ADP-ribose) polymer was observed in ischemic cerebral cortex 1hr after reperfusion (Fig. 8A). This poly (ADP-ribose) polymer formation was detected 6hr later (Fig. 8B), however, at 15hr following reperfusion, the formation was decreased to below detectable levels (data not shown). In the striatum, marked poly (ADP-ribose) polymer formation was also observed 1hr after reperfusion (Fig. 8C), and we confirmed that poly (ADP-ribose) polymer-positive cells were mostly neurons by morphological examination. To evaluate the PARP inhibitory effect of FR247304 in this model, sections of the cerebral cortex from 1hr after reperfusion were prepared. The formation of poly (ADP-ribose) polymer was strongly inhibited by administration of FR247304 at a dose of 32mg/kg (Fig. 8D).

***NAD depletion and effect of FR247304:*** NAD contents in the cerebral cortex and striatum were determined at 1, 3 and 24hr after ischemia-reperfusion. Marked NAD depletion was observed from 1hr after reperfusion in the cerebral cortex. In the striatum, significant decrease of NAD content was observed from 3hr after reperfusion (Fig. 9A). The NAD depletion after reperfusion was prevented by FR247304 treatment at a dose of 32mg/kg both in the cerebral cortex and in the striatum (Fig.9B). This result was consistent with that of PARP immunostaining, suggesting that FR247304 exerts neuroprotective effect on transient focal ischemia in rats via its potent PARP inhibition.

JPET Fast Forward. Published on April 9, 2004 as DOI: 10.1124/jpet.104.066944
This article has not been copyedited and formatted. The final version may differ from this version.


## Discussion

The aim of the present study was to evaluate the neuroprotective potential of a novel PARP-1 inhibitor FR247304, which was recently designed using X-ray analysis and a structure based drug design system, on ROS-mediated neuronal damage *in vitro* and on brain injury associated with transient focal ischemia-reperfusion in rats. FR247304 competes with NAD to inhibit at the catalytic site of PARP, consistent with the report that quinazolinone derivatives, including FR247304, tightly binds to the nicotinamide-ribose binding site (NI site) by hydrogen bonds (Ser904 and Gly863) and by a sandwich hydrophobic interaction (Tyr907 and Tyr869), and also that these compounds bind to the adenine-ribose binding site (AD site), in which known inhibitors do not bind (Kinoshita et al., 2004). Interestingly, FR247304 was more selective for PARP-1 than PARP-2 (10-fold higher selectivity) compared with non-selective general PARP-1 inhibitors such as 3-AB ($IC_{50}$ for PARP-1 = 11.2 μM and for PARP-2 = 9.8 μM, unpublished data) and PJ34 ($IC_{50}$ for PARP-1=110 nM and for PARP-2 = 86 nM, unpublished data). FR247304 also showed similar inhibitory activity both for human recombinant PARP and for rat brain PARP, suggesting that this compound can exert potent PARP-1 inhibitory activity in neuronal death models of rat origin tested in the present study, such as rat PC12 cells and a transient focal ischemia model in rats.

To determine PARP inhibitory properties and the neuroprotective properties of FR247304 in cultured cells, cell damage was induced by $H_2O_2$ exposure in PC12 cells and PARP activation was measured by NAD depletion. In our cell assay conditions, $H_2O_2$ exposure generated marked NAD reduction followed by severe cell damage. As expected given the potent PARP-1 inhibitory activity of FR247304, this compound

JPET Fast Forward. Published on April 9, 2004 as DOI: 10.1124/jpet.104.066944
This article has not been copyedited and formatted. The final version may differ from this version.


markedly attenuated both NAD depletion and cell damage, and the potency was consistent with its PARP-1 inhibitory activity in rat PARP enzyme assay. Other qunazolinone derivatives, which we have recently synthesized, showed an equivalent correlation between the potency in inhibiting PARP-1 activity and neuroprotective properties in cultured cells (Iwashita et al., unpublished data), suggesting that FR247304 possesses superior neuroprotective properties via its potent PARP-1 inhibitory activity combined with sufficient cell membrane permeability.

In addition to *in vitro* efficacy, FR247304 provides significant cerebroprotection following transient cerebral ischemia. Cerebral ischemia-reperfusion is accompanied by enhanced poly (ADP-ribosyl)ation (Endres et al., 1997; Tokime et al., 1998), and infarct volume is reduced by the administration of PARP inhibitors (Takahashi et al, 1997; Abdelkarim et al., 2001). The neuroprotective effects of PARP-1 inhibitors indicate that PARP play an important role in brain damage after transient ischemia. Consistent with the neuroprotective properties of other known PARP-1 inhibitors, FR247304 markedly reduced cortical infarct volume by 47% compared with vehicle treated control. The neuroprotective effect of FR247304 was more prominent in the cortex than in the striatum, in accordance with previous reports concerning neuroprotectants in stroke models (Lo et al., 1998; Schmid-Elsaesser et al., 2000; Furuichi et al., 2003; Iwashita et al., 2003) and also with our observation that NAD depletion in focal cerebral ischemia-reperfusion occurs predominantly in the cortex immediately after reperfusion, and that FR247304 treatment markedly attenuates NAD depletion. These results suggest that FR247304 exerted potent neuroprotective properties in focal ischemia model via its potent PARP-1 inhibitory activity, showing compatibility with results in the *in vitro* cell death model.

JPET Fast Forward. Published on April 9, 2004 as DOI: 10.1124/jpet.104.066944
This article has not been copyedited and formatted. The final version may differ from this version.


In focal ischemia models, nitric oxide and superoxide generation on reperfusion have been demonstrated (Nelson et al., 1992; Peters et al., 1998), and concomitant generation of these radicals can lead to formation of the strong oxidant peroxynitrite during reperfusion. Infarct volume after focal cerebral ischemia is reported to be reduced by overexpressing extracelluar SOD in mice (Sheng et al., 1998) and by the administration of free radical scavengers (Yamamoto et al., 1983; Yang et al., 2000; Iwashita et al., 2003). 7-Nitroindazole, a selective neuronal NOS inhibitor, has also been reported to ameliorate ischemic brain injury (Kamii et al., 1996; Gursoy-Ozdemir et al., 2000). These results raised the possibility that drugs which have a radical scavenging activity or neuronal NOS inhibitory activity could have a potential to attenuate the infarct volume induced by reperfusion following focal cerebral ischemia. However, in our *in vitro* assay, FR247304 showed no antioxidant property and nNOS inhibitory activity even at a concentration of $10^{-5}$M, indicating that FR247304 does not modulate the NO and/or ROS mediated pathway, but instead that the neuroprotective properties is likely due to the result from its specific PARP-1 inhibitory activity.

It has been proposed that PARP activation may be a late common step responsible for oxidative cell injury (Ha and Snyder, 1999) and PARP-induced cell death correlates well with cellular NAD depletion (Ying et al., 2001; Yu et al., 2002). NADPH oxidase and nNOS contribute to increased oxidative stress with subsequent activation of PARP, and NADPH oxidase inhibitor and nNOS inhibitors attenuate neuronal death without direct inhibition of PARP (Hwang et al., 2002). The DNA alkylating agent-induced NAD depletion is the cause of glycolytic failure and cell death after PARP activation, thus, the maintenance of NAD can mitigate cell death (Ying et al., 2003), suggesting that NAD depletion plays an essential role in the PARP-induced

JPET Fast Forward. Published on April 9, 2004 as DOI: 10.1124/jpet.104.066944
This article has not been copyedited and formatted. The final version may differ from this version.


cell death pathway. Consistent with these reports, neuroprotection by FR247304 observed in our study was the consequence of the maintenance of NAD by PARP inhibition, thus the activation of PARP could be causative factor and PARP inhibition is probably responsible for the neuroprotection in an oxidative neuronal death pathway.

As demonstrated by the pharamacokinetic study, the brain concentration of FR247304 at 32 mg/kg (i.p.) was found to be 0.75 μg/g at 1hr post dosing, the concentration which is calculated to be higher than $10^{-6}$M. Furthermore, even at 6hr following drug administration, the brain concentration was sustained at the level of half maximum concentration (Cmax), which is estimated as about $10^{-6}$M. This dosing regimen yielded high brain levels of FR247304 to sufficiently inhibit PARP-1 inhibitory activity in the brain. As expected from a good pharmacokinetic profile, treatment with FR247304 prior to the ischemia-reperfusion insult produced robust and significant neuroprotection, suggesting that ischemia-reperfusion induced PARP activation persists for some time, and that the neuroprotective effects of FR247304 presumably are related to its PARP-1 inhibiting properties. The present study showed the temporal pattern of brain PARP activation following ischemia demonstrating that PARP activation evaluated by poly (ADP-ribose) polymer formations were sustained from immediately after reperfusion to 6hr later, and then the formation was decreased to below detectable levels at 15hr following reperfusion.

While the putative mechanism of neuroprotection by FR247304 is PARP-1 inhibition, infarct volume can also be reduced by improving rCBF. However, there was no enhancement of rCBF to cortical area of the infarct in 10 and 32mg/kg FR247304-treated rat as assessed by rCBF monitored during the MCA occlusion and monitoring period. Therefore, it is unlikely that any heomodynamic actions of

FR247304 contributed to the neuroprotective action via improvement of rCBF. Furthermore, reductions of infarct volume and neurological deficits in PARP deficient mice or in mice treated with the PARP-1 inhibitor 3-AB does not depend on changes in CBF, but rather are correlated with reduced PARP activation in ischemic brain tissue (Eliasson et al., 1997; Endres et al., 1997). Moreover, although hypothermia can also reduce infarct volume, body temperature does not change following ischemia-reperfusion in PARP deficient mice (Onesti et al., 1991; Chen et al., 1992; Eliasson et al., 1997). As FR247304 treatment did not influence body temperature in the present study, the beneficial effects of this compound are unlikely to result from the hypothermic activity.

Several classes of competitive PARP-1 inhibitors have been reported to date and treatment with PARP-1 inhibitors such as 3-AB or PJ34 reportedly decreased ischemic injury in a rat model of MCA occlusion (Endres et al., 1997; Abdelkarim et al., 2001). In the present study, we have compared the potency and neuroprotective efficacy of these reference PARP inhibitors with FR247304 in a PARP-1 enzyme assay, a cell death assay and a rat transient focal ischemia model. FR247304 showed the most potent PARP inhibitory activity compared to 3-AB and PJ34, and the rank order of their cytoprotective properties against $H_2O_2$-induced cell death paralleled their PARP inhibitory actions. In our in vivo experimental design, FR247304 treatment (32mg/kg, i.p.) exerted robust reduction in infarct volume by 47%, and was more efficacious than those of 3-AB and PJ34 treatment. There is a report demonstrating that an intravenous administration of PJ34 markedly reduced infarct volume by over 70% (Abdelkarim et al., 2001), raising the possibility that intravenous administration might provide a high brain concentration, and thus, the extent of neuroprotection may depend on the paradigm differences (e.g. administration route and time point).

JPET Fast Forward. Published on April 9, 2004 as DOI: 10.1124/jpet.104.066944
This article has not been copyedited and formatted. The final version may differ from this version.


Furthermore, although we have observed a dose-dependent neuroprotection with FR247304 treatment, PJ34 showed a bell-shaped dose-response relationship for its protective actions and it lost the efficacy at a higher dose (10mg/kg, i.p., 17% reduction), being consistent with a case of another PARP inhibitor DPQ (Takahashi et al., 1997). While 3-AB reduced infarct volume from relatively low dose (32mg/kg) in spite of its low potency but with additional effects, higher dosing (100mg/kg) was less neuroprotective. As it is not clear why high doses of PARP-1 inhibitors are less neuroprotective, extensive investigations could be required if excessive PARP inhibition induces cell death and low selective compound possessing secondary effects can affect cell death/survival. Our comparative studies taken together indicate that FR247304 exerts significant and dose-dependent neuroprotection on brain injury associated with focal brain ischemia, consistent with other PARP-1 inhibitors in previous reports (Endres et al., 1997; Takahashi et al., 1997). However, considering with the reduction of brain infarction size following focal ischemia in PARP-1 deficient mice (Eliasson et al., 1997) and also that FR247304 possessed a superior potential on PARP inhibitory activity *in vitro*, the efficacy and potency of FR247304 in focal ischemia *in vivo* were below expectations. Therefore, it would warrant further detailed studies to address efficacy with intravenous administration, specificity, cell permeability and pharmacokinetic property of each drug.

In conclusion, a newly synthesized PARP-1 inhibitor, FR247304, exhibited potent PARP-1 inhibition both *in vitro* and *in vivo*, with significant neuroprotective properties following ischemia-reperfusion in rats, suggesting that this compound and/or a water-soluble derivative of FR247304 could be not only an important tool for investigation of the physiological role of PARPs in neurodegenerative pathways, but also an attractive therapeutic candidate for stroke and neurodegenerative disease.

**Acknowledgments**

We thank Dr. Raymond D. Price for his helpful comments in preparing the manuscript.

## References

Abdelkarim GE, Gertz K, Harms C, Katchanov J, Dirnagl U, Szabo C and Endres M (2001) Protective effects of PJ34, a novel, potent inhibitor of poly(ADP-ribose) polymerase (PARP) in in vitro and in vivo models of stroke. *Int. J. Mol. Med.* 7(3): 255-260

Banasik M, Komura H, Shimoyama M, and Ueda K (1992) Specific inhibitors of poly(ADP-ribose) synthetase and mono(ADP-ribosyl)transferase. *J Biol Chem* 267:1569-1575

Buege JA and Aust SD (1978) Microsomal lipid peroxidation. *Methods Enzymol* 52: 302-310

Callaway JK, Beart PM and Jarrott B (1998) A reliable procedure for comparison of antioxidants in rat brain homogenates. *J Pharmacol Toxicol Methods* 39(3): 155-162

Chan PH (1996) Role of oxidation in ischemic brain damage. *Stroke* 27:1124-1129

Chen H, Chopp M, Zhang ZQ and Garcia JH (1992) The effect of hypothermia on transient middle cerebral artery occlusion in the rat. *J. Cereb Blood Flow Metab.* 12(4): 621-628

Coyle JT and Puttfarchen P (1993) Oxidative stress, glutamate, and neurodegenerative disorders. *Science* 262:689-695

Cosi C, Colpaert F, Koek W, Degryse A, and Marien M (1996) Poly (ADP-ribose) polymerase inhibitors protect against MPTP-induced depletions of striatal dopamine and cortical noradrenaline in C57BL/6 mice. *Brain Res* 729:264-269

Eliasson MJ, Sampei K, Madier AS, Hurn PD, Traystman RJ, Bao J, Pieper A, Wang ZQ, Dawson TM, Snyder SH and Dawson VL (1997) Poly (ADP-ribose)

JPET Fast Forward. Published on April 9, 2004 as DOI: 10.1124/jpet.104.066944
This article has not been copyedited and formatted. The final version may differ from this version.


polymerase gene disruption renders mice resistant to cerebral ischemia. *Nature Med.* 3(10): 1089-1095

Endres M, Wang ZQ, Namura S, Waeber C and Moskowitz MA (1997) Ischemic brain injury is mediated by the activation of poly (ADP-ribose) polymerase. *J. Cereb Blood Flow Metab.* 17(11):1143-1151

Endres M, Scott G, Namura S, Salzman AL, Huang PL, Moskowitz MA and Szabo C (1998) Role of peroxynitrite and neuronal nitric oxide synthase in the activation of poly(ADP-ribose) synthetase in a murine model of cerebral ischemia-reperfusion. *Neurosci. Lett.* 248(1): 41-44

Facchinetti F, Dawson VL and Dawson TM (1998) Free radicals as mediators of neuronal injury. *Cell Mol. Neurobiol.* 18:667-682

Furuichi Y, Katsuta K, Maeda M, Ueyama N, Moriguchi A, Matsuoka N, Goto T and Yanagihara T (2003) Neuroprotective action of tacrolimus (FK506) in focal and global cerebral ischemia in rodents: dose dependency, therapeutic time window and long-term efficacy. *Brain Res.* 965:137-145

Gursoy-Ozdemir Y, Bolay H, Saribas O and Dalkara T (2000) Role of endotherial nitric oxide generation and peroxynitrite formation in reperfusion injury after focal cerebral ischemia. *Stroke* 31(8): 1974- 1980

Ha HC and Snyder SH (1999) Poly (ADP-ribose) polymerase is a mediator of necrotic cell death by ATP depletion. *Proc. Natl. Acad. Sci. USA* 96: 13978-13982

Huang PL, Dawson TM, Bredt DS, Snyder SH and Fishman MC (1993) Targeted disruption of the neuronal nitric oxide synthase gene. *Cell* 75:1273-1286

Hwang JJ, Choi SY and Koh JY (2002) The role of NADPH oxidase, neuronal nitric oxide synthase and poly(ADP-ribose) polymerase in oxidative neuronal death induced in cortical cultures by brain-derived neurotrophic factor and

neurotrophin-4/5. *J. Neurochem.* 82:894-902

Iwashita A, Maemoto T, Nakada H, Shima I, Matsuoka N and Hisajima H (2003) A novel potent radical scavenger, 8-(4-Fluorophenyl)-2-((2E)-3-phenyl-2-propenoyl)-1,2,3,4-tetrahydropyrazolo[5,1-c][1,2,4]triazine(FR210575), prevents neuronal cell death in cultured primary neurons and attenuated brain injury after focal ischemia in rats. *J. Pharmacol. Exp. Ther.* 307: 961-968

Iwashita A, Yamazaki S, Mihara K, Hattori K, Yamamoto H, Ishida J, Matsuoka N and Mutoh S (2004) Neuroprotective effects of novel poly (ADP-ribose) polymerase-1 inhibitor, 2-{3-[4-(4-chlorophenyl)-1-piperazinyl]propyl}-4(3H)-quinazolinone (FR255595), in an in vitro model of cell death and in mouse MPTP model of parkinson's disease. *J. Pharmacol. Exp. Ther.* : In press

Kamii H, Mikawa S, Murakami K, Kinouchi H, Yoshimoto T, Reola L, Carison E, Epstein CJ and Chan PH (1996) Effects of nitric oxide synthase inhibition on brain infarction in SOD-1-transgenic mice following transient focal cerebral ischemia. *J Cereb. Blood Flow Metab.* 16(6):1153-1157

Kinoshita T, Nakanishi I, Warizawa M, Iwashita A, Kido Y, Hattori K and Fujii T (2004) Inhibitor-induced structural change of the active site of human poly (ADP-ribose) polymerase. *FEBS Lett*. 556(1-3): 43-46

Lahiri DK and Ge Y (2000) Electrophoretic mobility shift assay for the detection of specific DNA-protein complex in nuclear extracts from the cultured cells and frozen autopsy human brain tissue. *Brain Res Protocols* 5 (3):257-265

LaPlaca MC, Zhang J, Raghupathi R, Li JH, Smith F, Bareyre FM, Snyder SH, Graham DI and McIntosh TK (2001) Pharmacologic inhibition of poly (ADP-ribose) polymerase is neuroprotective following traumatic brain injury in rats. *J Neurotrauma* 18(4):369-376

Lo EH, Bosque-Hamilton P and Meng W (1998) Inhibition of poly(ADP-ribose) polymerase: reduction of ischemic injury and attenuation of N-methyl-D-aspartate-induced neurotransmitter dysregulation. *Stroke* 29(4):830-836

Nelson CW, Wei EP, Povlishock JT, Kontos HA and Moskowitz MA (1992) Oxygen radicals in cerebral ischemia. *Am. J. Physiol* 263: H1356-H1362

Onesti ST, Baker CJ, Sun PP and Solomon RA (1991) Transient hypothermia reduces focal ischemia brain injury in the rat. *Neurosurgery* 29(3): 369-373

Peters O, Back T, Lindauer U, Busch C, Megow D, Dreier J and Dirnagl U (1998) Increased formation of reactive oxygen species after permanent and reversible middle cerebral artery occlusion in the rat. *J. Cereb. Blood Flow Metab.* 18(2):196-205

Schmid-Elsaesser R, Hungerhuber E, Zausinger S, Baethmann A and Reulen HJ (2000) Neuroprotective effects of the novel brain-penetrating antioxidant U-101033E and the spin-trapping agent $\alpha$-phenyl-*N-tert*-butyl nitrone (PBN). *Exp Brain Res.* 130: 60-66

Sheng H, Bart RD, Oury TD, Pearlstein RD, Crapo JD and Warner DS (1998) Mice overexpressing extracellular superoxide dismutase have increased resistance to focal cerebral ischemia. *Neuroscience* 88:185-191

Siesjo BK, Agardh CD and Bengtsson F (1989) Free radials and brain damage. *Cerebrovasc. Brain Metab. Rev.* 1: 165-211

Szabo C, Zingarelli B, O'Connor M and Salzman AL (1996) DNA strand breakage, activation of poly (ADP-ribose) synthetase, and cellular energy depletion are involved in the cytotoxicity of macrophages and smooth muscle exposed to peroxynitrite. *Proc. Natl. Acad. Sci. U.S.A.* 93: 1753-1758

Takahashi K, Greenberg JH, Jackson P, Maclin K and Zhang J (1997) Neuroprotective effects of inhibiting poly(ADP-ribose) synthetase on focal cerebral ischemia in rats. *J. Cereb Blood Flow Metab.* 17(11):1137-1142

Tokime T, Nozaki K, Sugino T, Kikuchi H, Hashimoto N and Ueda K (1998) Enhanced poly(ADP-ribosyl)ation after focal ischemia in rat brain. *J. Cereb. Blood Flow Metab.* 18: 991-997

Yamamoto M, Shima T, Uozumi T, Sogabe T, Yamada K and Kawasaki T (1983) A possible role of lipid peroxidation in cellular damages caused by cerebral ischemia and the protective effect of alpha-tocopherol administration. *Stroke* 14:977-982

Yang Y, Li Q and Shuaib A (2000) Neuroprotection by 2-h postischemia administration of two free radical scavengers, $\alpha$-phenyl-n-tert-butyl-nitrone (PBN) and N-tert-butyl-(2-sulfophenyl)-nitrone (S-PBN), in rats subjected to focal embolic cerebral ischemia. *Exp. Neurology* 163:39-45

Ying W, Sevigny MB, Chen Y and Swanson RA (2001) Poly (ADP-ribose) glycohydrolase mediates oxidative and excitotoxic neuronal death. *Proc. Natl. Acad. Sci. U.S.A.* 98: 12227-12232

Ying W, Garnier P and Swanson RA (2003) NAD+ repletion prevents PARP-1-induced glycolytic blockade and cell death in cultured mouse astrocytes. *Biochem. Biophys. Res. Commun* 308:809-813

Yu SW, Wang H, Poitras MF, Coombs C, Bowers WJ, Federoff HJ, Poirier GG, Dawson TM and Dawson VL (2002) Mediation of poly (ADP-ribose) polymerase-1-dependent cell death by apoptosis-inducing factor. *Science* 297: 259-263

Zhang J, Dawson VL, Dawson TM and Snyder SH (1994) Nitric oxide activation of

poly(ADP-ribose) synthetase in neurotoxicity. *Science* 263: 687-689

JPET Fast Forward. Published on April 9, 2004 as DOI: 10.1124/jpet.104.066944
This article has not been copyedited and formatted. The final version may differ from this version.


## Figure legends

Figure 1

Chemical structure of FR247304, 5-chloro-2-[3-(4-phenyl-3,6-dihydro-1(2H)-pyridinyl) propyl]-4(3H)-quinazolinone

Figure 2

Enzyme kinetics analysis of PARP inhibition by FR247304. Lineweaver-Burk plot analysis shows that the inhibitory action of FR247304 is competitive (A). Dixon plot analysis demonstrates that the Ki value of FR247304 is 35nM (B).

Figure 3

Inhibitory activity and specificity of FR247304. PARP inhibitory activity of FR247304 in human recombinant PARP was compared with that in rat and mouse PARP. $IC_{50}$ values were calculated from the concentration dependence of the inhibition curves using computer-assisted non-linear regression analyses (A). Comparison of inhibitory activities between FR247304 and positive control for Vitamin E in the TBARS assay (B) and 7-nitroindazole in the NOS assay (C). FR247304 did not exhibit radical scavenging activity nor NOS inhibitory activity at a concentration from $10^{-8}$ to $10^{-5}$M in either assay. Values are means ± S.E.M. of n=2-3 determinations tested in triplicate.

Figure 4

Hydrogen peroxide-induced NAD depletion and cell death was attenuated by PARP inhibition with FR247304 treatment in PC12 cells. Exposure of 100μM $H_2O_2$ for 30 min induced marked NAD depletion. FR247304 at concentrations from $10^{-8}$M attenuated NAD depletion, and at a $10^{-5}$M FR247304 prevented NAD depletion completely (A).

JPET Fast Forward. Published on April 9, 2004 as DOI: 10.1124/jpet.104.066944
This article has not been copyedited and formatted. The final version may differ from this version.


Exposure of 100μM $H_2O_2$ for 6hr produced severe cell damage as evaluated by LDH release assay. This damage was significantly reduced by addition of $10^{-8}$ to $10^{-5}$M FR247304 0.5hr prior to $H_2O_2$ exposure to the culture medium (B). Each point represents the means ± S.E.M. of at least three experiments. *, P<0.05, **, P<0.01 versus vehicle treated control group (by one-way ANOVA followed by Dunnett's multiple comparison test). ##, P<0.01 versus vehicle treated control group (by Student's t-test).

Figure 5

The plasma and brain concentrations of FR247304 in rats were determined at 0.5, 1, 2, 4 and 6hr following intraperitoneal administration at 32 mg/kg. Mean plasma (triangles) and brain (circles) concentration of Cmax (1h after dosing) were 0.15μg/ml and 0.74μg/g tissue, respectively, and the brain/plasma concentration ratio was 4.35. Data are presented as mean ± S.E.M. values (n=3 per each time point).

Figure 6

Neuroprotective effects of FR247304 on brain damage induced by transient MCA occlusion in rats. FR247304 was administered intraperitoneally at a dose of 10 or 32 mg/kg twice at 10min prior to MCA occlusion and 10min prior to reperfusion. Representative coronal sections of vehicle-treated (left) and FR247304-treated (right) rats brains after staining with cresyl violet (A). Brain infarct size (B) and cortical infarct size of 2-mm coronal sections (C) were reduced by FR247304 treatment compared with vehicle treatment. Data are presented as mean ± S.E.M. values (n=9 per experimental condition). *, P<0.05 and **, P<0.01 by one-way ANOVA followed by Dunnett's multiple comparison test.

JPET Fast Forward. Published on April 9, 2004 as DOI: 10.1124/jpet.104.066944
This article has not been copyedited and formatted. The final version may differ from this version.


Figure 7

Effect of FR247304 on body temperature following transient MCA occlusion in rats. MCA occlusion for 90min resulted in increased body temperature. FR247304 treatment (10 or 32mg/kg, i.p.) had no influence on body temperature at 1.5hr after occlusion and 24hr after reperfusion. Data are presented as mean ± S.E.M. values (n=9 per experimental condition).

Figure 8

Representative photographs of poly (ADP-ribose) polymer immunostaining after focal brain ischemia in rats. Poly (ADP-ribose) immunoreactivity was markedly increased in cerebral cortex and striatum from 1hr to 6hr after reperfusion following 1.5hr MCA occlusion. Red stained cells show poly(ADP-ribose) polymer positive cells. Formation of poly (ADP-ribose) polymer was detected at 1hr after reperfusion in cerebral cortex (A), and also at 6hr later (B). In the striatum, marked poly (ADP-ribose) polymer formation was observed at 1hr after reperfusion (C). FR247304 administration (32mg/kg) twice by i.p. at 10min prior to MCA occlusion and 10min prior to reperfusion markedly inhibited the formation of poly (ADP-ribose) polymer in cerebral cortex 1hr after reperfusion (D).

Figure 9

Cellular NAD contents in the cerebral cortex and the striatum at 1, 3 and 24hr after reperfusion following 90min MCA occlusion in rats (A). FR247304 administration (32mg/kg) twice by i.p. at 10min prior to MCA occlusion and 10min prior to reperfusion significantly attenuated NAD depletion at 3hr after reperfusion both in the cerebral

cortex and the striatum (B). Data are presented as mean ± S.E.M. values (n=5-6 per experimental condition). **, P<0.01 versus vehicle treated control group (one-way ANOVA followed by Dunnett's multiple comparison test). ##, P<0.01 versus vehicle treated control group (by Student's t-test).

JPET Fast Forward. Published on April 9, 2004 as DOI: 10.1124/jpet.104.066944
This article has not been copyedited and formatted. The final version may differ from this version.


TABLE 1

Pharmacological properties of 3-AB and PJ34 on PARP inhibitory activity, cytoprotective activity in PC12 cells and neuroprotective actions in rat focal cerebral ischemia. PARP inhibitory activity was evaluated in human recombinant PARP. $IC_{50}$ values were calculated from the concentration dependence of the inhibition curves by using computer-assisted non-linear regression analyses. Values are means ± S.E.M. of n=2 determinations tested in triplicate. To determine cytoprotective potential of 3-AB and PJ34, $H_2O_2$-induced cell death was evaluated by using LDH assay. 3-AB and PJ34 significantly and concentration-dependently attenuated cell death at a concentration from $10^{-4}$ to $10^{-2}$M and from $10^{-7}$ to $10^{-5}$M, respectively. Values are means ± S.E.M. of n=2 determinations tested in triplicate. *, P<0.05, **, P<0.01 versus vehicle treated control group (by one-way ANOVA followed by Dunnett's multiple comparison test). ##, P<0.01 versus vehicle treated control group (by Student's t-test). In rat transient ischemia model, 3-AB and PJ34 were evaluated at a dose of 100mg/kg or at the doses of 3.2 and 10mg/kg, respectively. 3.2mg/kg dosing of PJ34 significantly reduced cortical damage by 33%, however, 10mg/kg dosing showed reversed effect (17% reduction). Values are means ± S.E.M. of N=9 rats. * P<0.05 by one-way ANOVA followed by Dunnett's multiple comparison test.

JPET Fast Forward. Published on April 9, 2004 as DOI: 10.1124/jpet.104.066944
This article has not been copyedited and formatted. The final version may differ from this version.



TABLE 1

Pharmacological properties of other PARP inhibitors

| Drug | PARP inhibitory activity ($IC_{50}$) | $H_2O_2$-induced cell death in PC12 | | Rat focal ischemia model | | |
|---|---|---|---|---|---|---|
| | | LDH assay | | Dose (mg/kg) | Cortical infarct size ($mm^2$) | % of recovery |
| | | Drug conc. | $OD_{560nm}$ | | | |
| 3-AB | 11200±810 nM | (-) | 0.204±0.009 ## | vehicle | 128.97±13.81 | - |
| | | vehicle | 0.732±0.015 | 32 | 105.68±11.04 | 18% |
| | | $10^{-5}$M | 0.706±0.012 | 100 | 114.65±12.98 | 11% |
| | | $10^{-4}$M | 0.541±0.021 ** | | | |
| | | $10^{-3}$M | 0.427±0.011 ** | | | |
| | | $10^{-2}$M | 0.357±0.008 ** | | | |
| PJ34 | 110±1.9 nM | (-) | 0.194±0.005 ## | vehicle | 126.73±14.16 | - |
| | | vehicle | 0.719±0.012 | 3.2 | 85.04± 9.21 * | 33% |
| | | $10^{-8}$M | 0.668±0.022 | 10 | 105.27±10.33 | 17% |
| | | $10^{-7}$M | 0.557±0.019 ** | | | |
| | | $10^{-6}$M | 0.406±0.011 ** | | | |
| | | $10^{-5}$M | 0.367±0.013 ** | | | |

**Figure. 1**



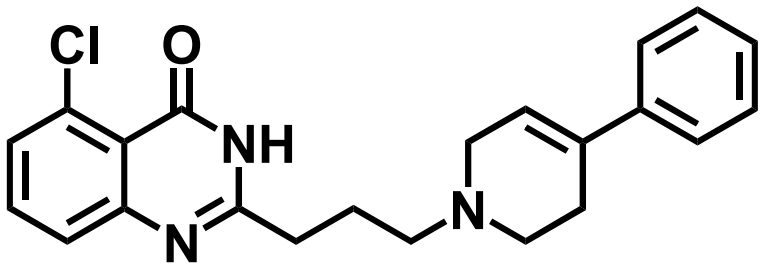

JPET Fast Forward. Published on April 9, 2004 as DOI: 10.1124/jpet.104.066944
This article has not been copyedited and formatted. The final version may differ from this version.

**Figure 2**



**A. Lineweaver-Burk Plot**

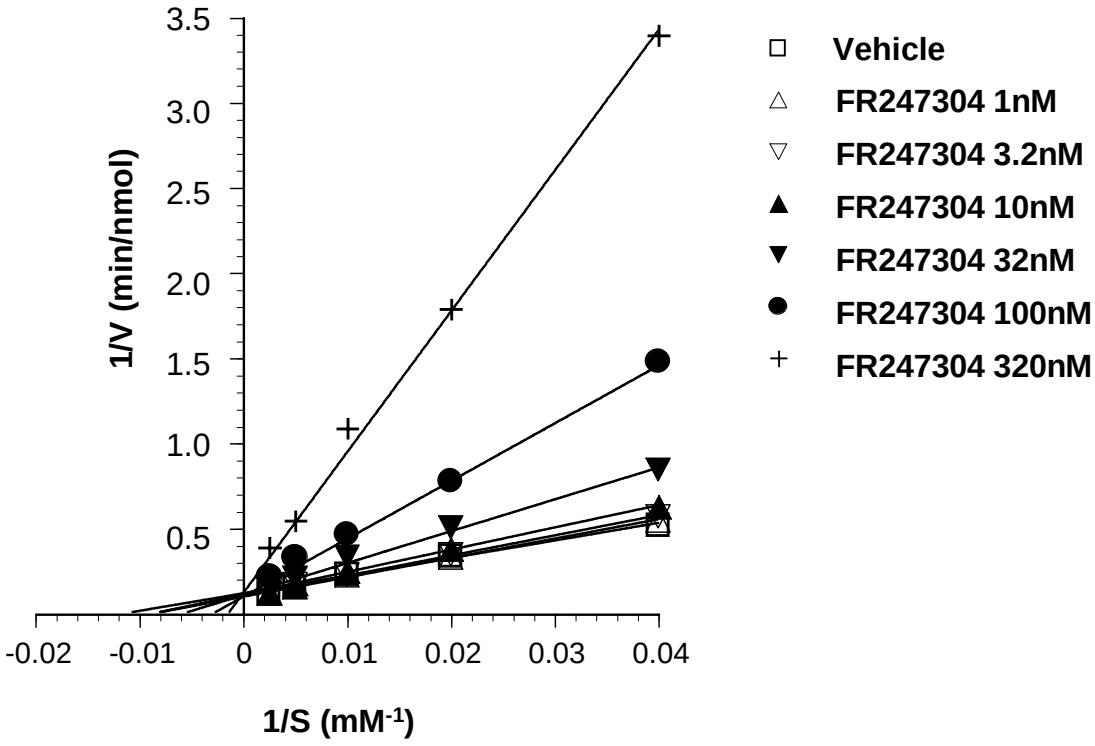


**B. Dixon Plot**

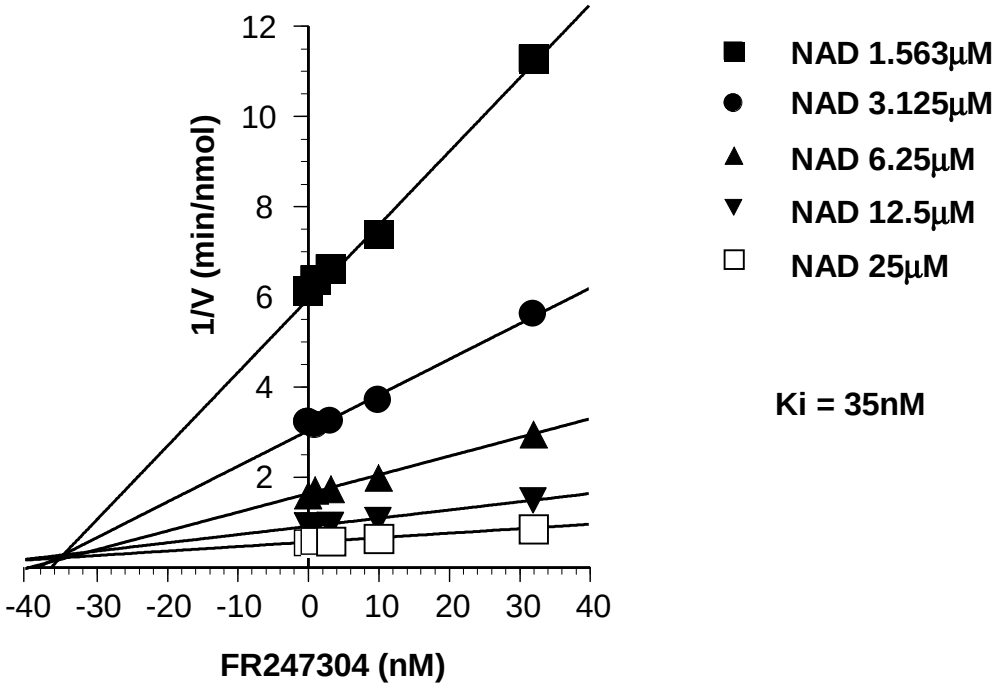

JPET Fast Forward. Published on April 9, 2004 as DOI: 10.1124/jpet.104.066944
This article has not been copyedited and formatted. The final version may differ from this version.

**Figure 3**



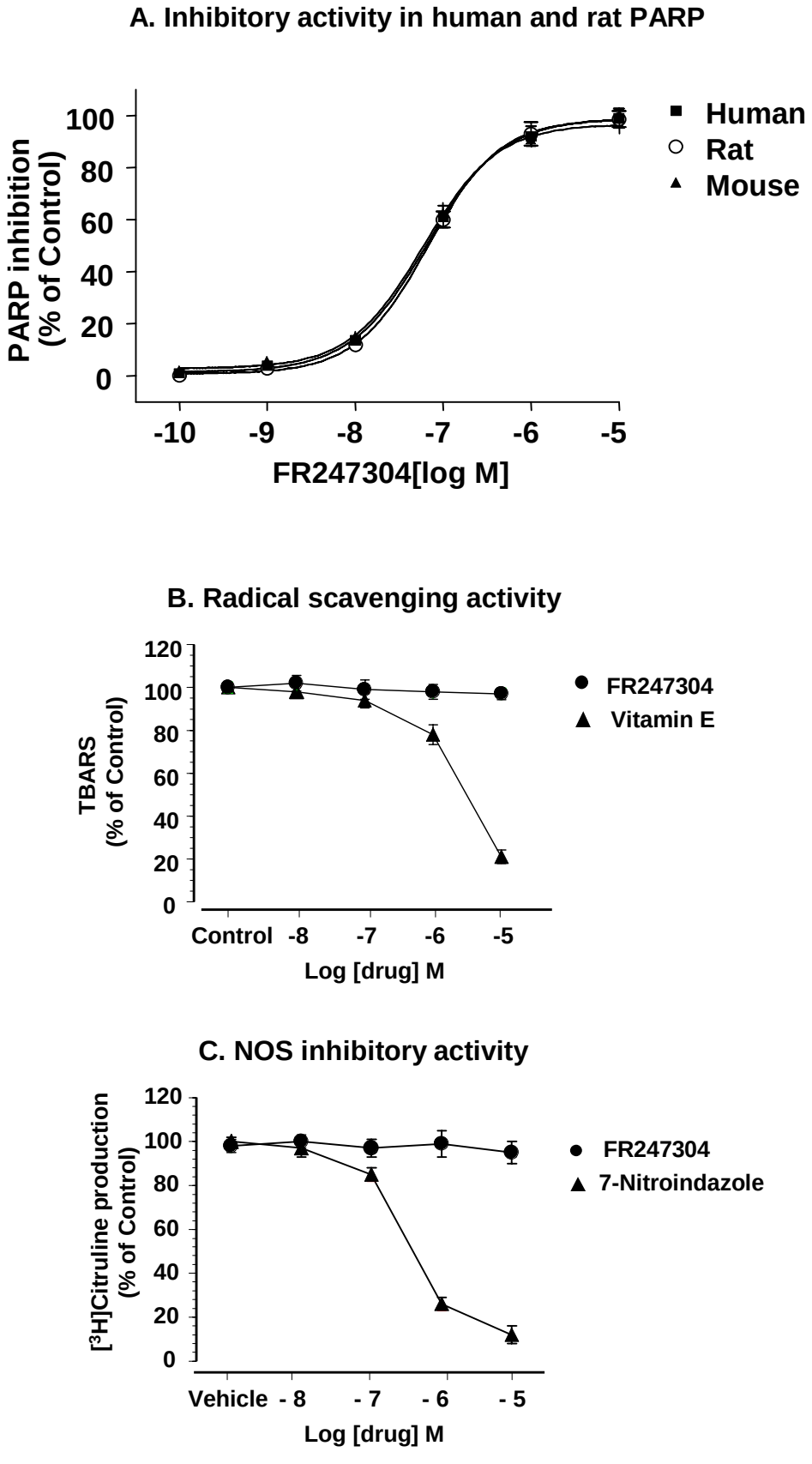

JPET Fast Forward. Published on April 9, 2004 as DOI: 10.1124/jpet.104.066944
This article has not been copyedited and formatted. The final version may differ from this version.

**Figure 4**



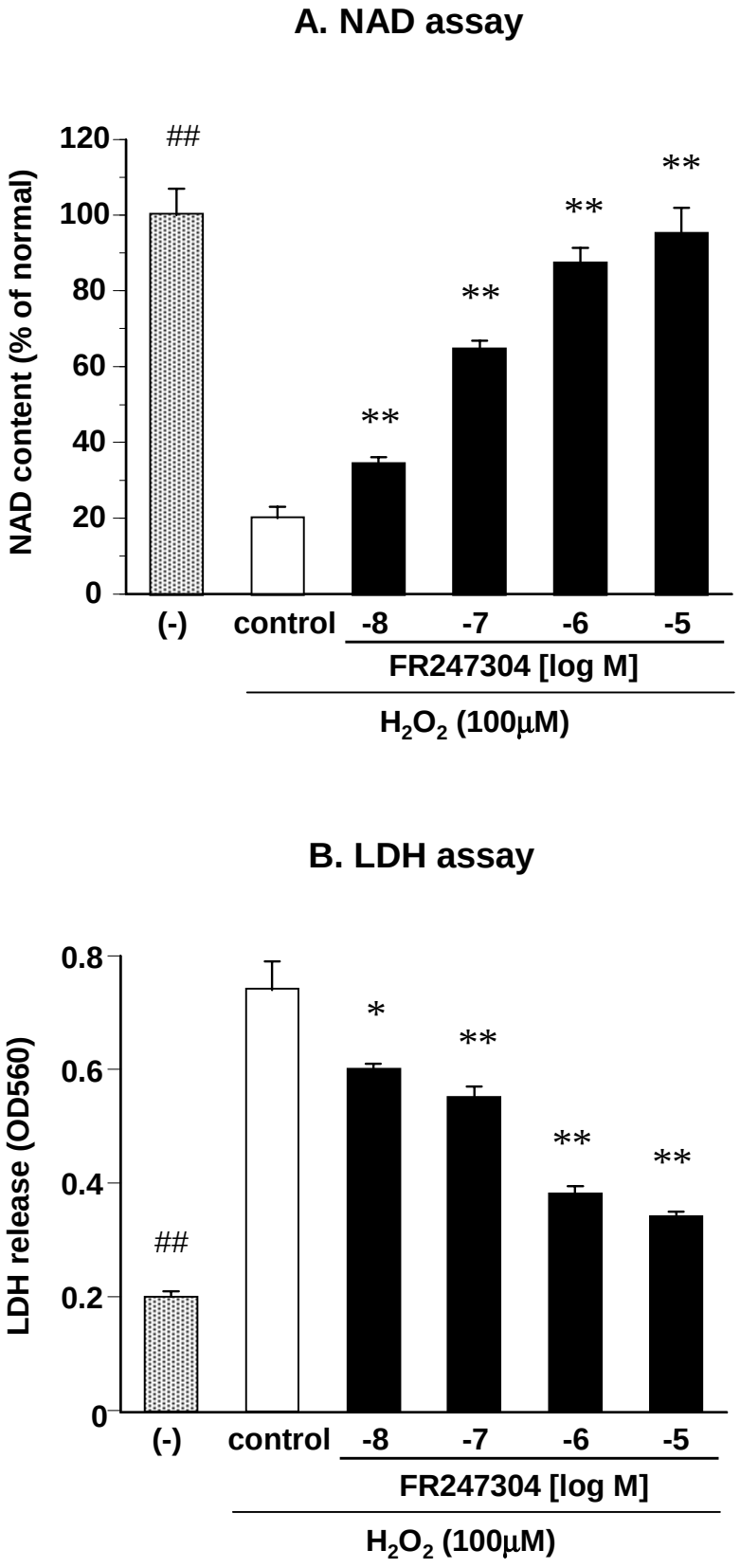

JPET Fast Forward. Published on April 9, 2004 as DOI: 10.1124/jpet.104.066944
This article has not been copyedited and formatted. The final version may differ from this version.

**Figure 5**



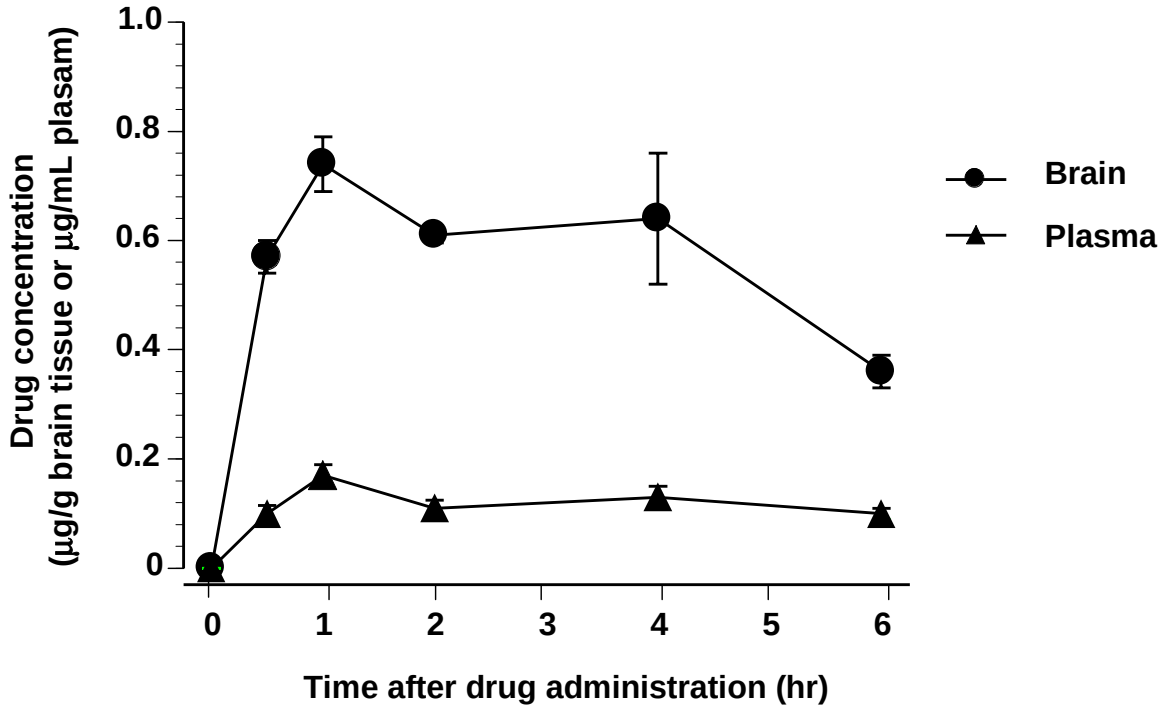

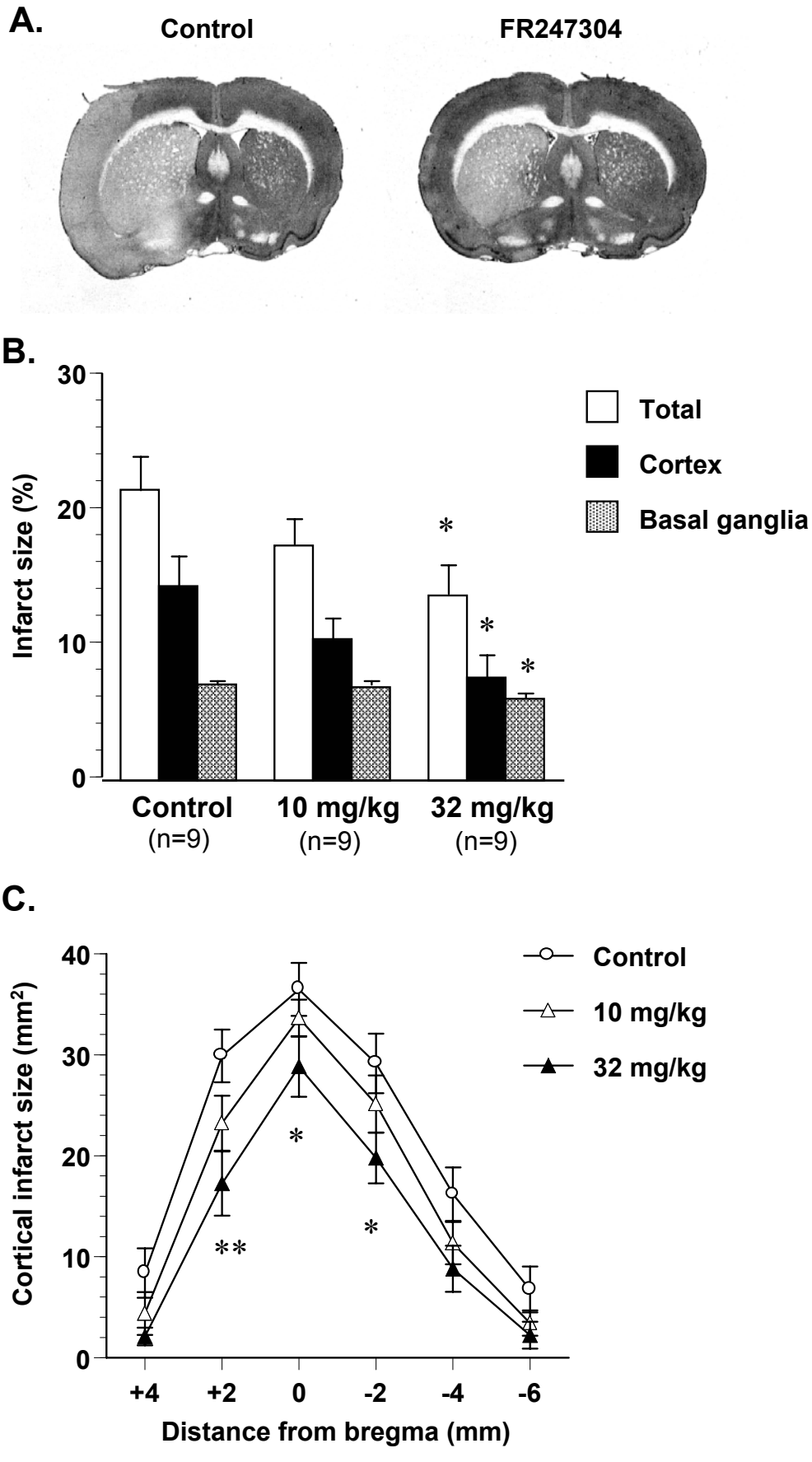
A.
Control
FR247304
B.
Infarct size (%)
30
20
10
0
Total
Cortex
Basal ganglia
*
*
*
Control
(n=9)
10 mg/kg
(n=9)
32 mg/kg
(n=9)
C.
Cortical infarct size (mm²)
40
30
20
10
0
Control
10 mg/kg
32 mg/kg
**
*
*
+4
+2
0
-2
-4
-6
Distance from bregma (mm)

JPET Fast Forward. Published on April 9, 2004 as DOI: 10.1124/jpet.104.066944
This article has not been copyedited and formatted. The final version may differ from this version.

**Figure 7**



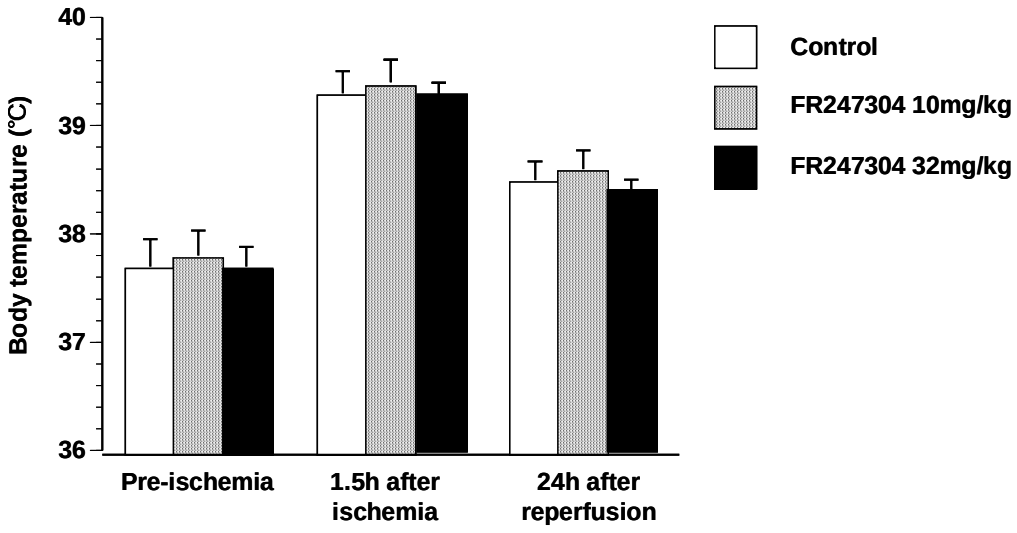

JPET Fast Forward. Published on April 9, 2004 as DOI: 10.1124/jpet.104.066944
This article has not been copyedited and formatted. The final version may differ from this version.

**Figure 8**



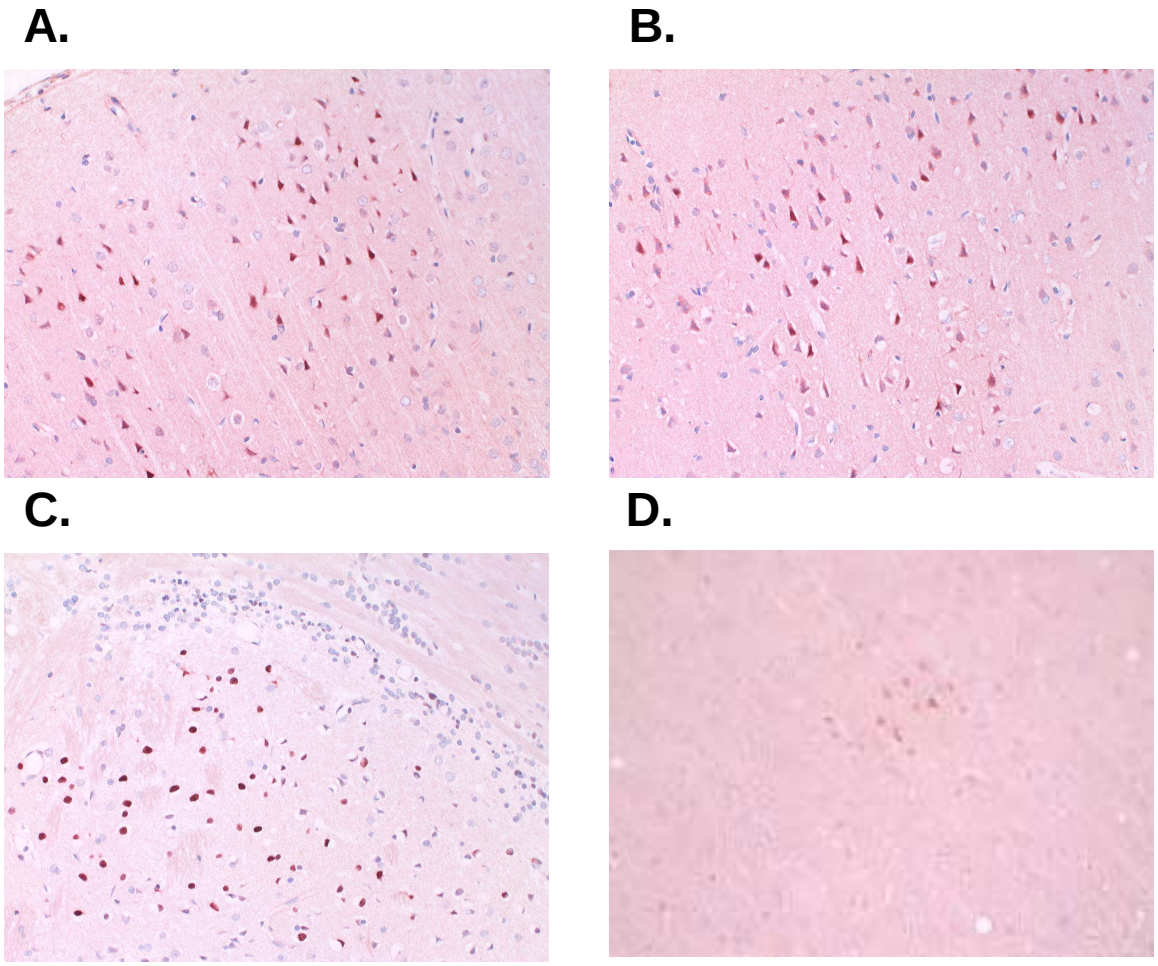


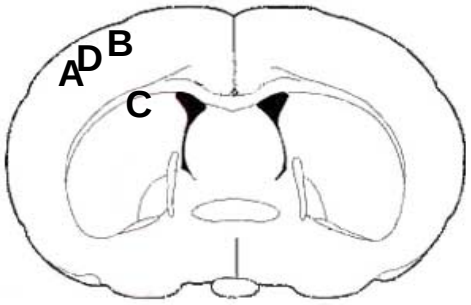


**A. 1hr after reperfusion in cerebral cortex**

**B. 6hr after reperfusion in the cerebral cortex**

**C. 1hr after reperfusion in the striatum**

**D. 1hr after reperfusion in cerebral cortex**

**+ FR247304 (32mg/kg)**

JPET Fast Forward. Published on April 9, 2004 as DOI: 10.1124/jpet.104.066944
This article has not been copyedited and formatted. The final version may differ from this version.

**Figure 9**

Fig.9 JPET#66944